© 2001 Nature Publishing Group http://structbio.nature.com

Tuning of chaperone activity of Hsp70 proteins by modulation of nucleotide exchange

Dirk Brehmer[1], Stefan Rüdiger[1,2], Claudia S. Gässler[1], Dagmar Klostermeier[3,4], Lars Packschies[4], Jochen Reinstein[4], Matthias P. Mayer[1] and Bernd Bukau[1]

[1]*Institut für Biochemie und Molekularbiologie, Albert-Ludwigs-Universität Freiburg, Hermann-Herder-Str. 7, D-79104 Freiburg, Germany.* [2]*Cambridge Centre for Protein Engineering, MRC Centre, Hills Road, Cambridge CB2 2QH, UK.* [3]*The Scripps Research Institute, Department of Molecular Biology, MB-19, 10550 North Torrey Pines Road, La Jolla, California 92037, USA.* [4]*Max-Planck-Institut für molekulare Physiologie, Abteilung physikalische Biochemie, Otto-Hahn-Str. 11, D-44227 Dortmund, Germany.*

The Hsp70 chaperone activity in protein folding is regulated by ATP-controlled cycles of substrate binding and release. Nucleotide exchange plays a key role in these cycles by triggering substrate release. Structural searches of Hsp70 homologs revealed three structural elements within the ATPase domain: two salt bridges and an exposed loop. Mutational analysis showed that these elements control the dissociation of nucleotides, the interaction with exchange factors and chaperone activity. Sequence variations in the three elements classify the Hsp70 family members into three subfamilies, DnaK proteins, HscA proteins and Hsc70 proteins. These subfamilies show strong differences in nucleotide dissociation and interaction with the exchange factors GrpE and Bag-1.

Hsp70 chaperones undergo ATP-induced conformational changes that determine their affinity for substrates[1,2]. ATP bound to the N-terminal ATPase domain lowers the affinity of Hsp70 for substrates, presumably through opening of the C-terminal substrate binding cavity. ATP hydrolysis populates the closed state of the substrate binding cavity, thereby trapping associated substrates[3,4]. This step is regulated by DnaJ cochaperones that couple ATP hydrolysis with substrate binding. ADP release is rate-limiting for substrate release. ADP dissociation is further decreased by physiological concentrations of P_i. ATP binds to the nucleotide-free chaperone through rapid initial association (step 1, initial encounter complex, DnaK*–ATP), followed by slow isomerization (step 2, tightly bound complex, DnaK–ATP), which is kinetically coupled to substrate release[5–9].

$$\text{DnaK} + \text{ATP} \overset{\text{step 1}}{\rightleftharpoons} \text{DnaK*–ATP} \overset{\text{step 2}}{\rightleftharpoons} \text{DnaK–ATP}$$

For the *Escherichia coli* homolog, DnaK, ADP dissociation is strongly stimulated up to 5,000-fold by its cochaperone GrpE acting as a nucleotide exchange factor[10,11]. It has been debated whether members of the Bag protein family are nucleotide exchange factors for eukaryotic Hsp70/Hsc70[12,13]. Bag proteins are a heterogeneous family of multidomain proteins that share the Bag domain and are implicated in the nucleotide exchange reaction[14]. Bag proteins such as Bag-1 play roles in the regulation of signal transduction proteins, transcription factors and proteolysis. In a more general context, the extent of how the nucleotide exchange reaction and its regulation by exchange factors is subjected to evolutionary variation within the Hsp70 family remains unclear. In order to dissect the nucleotide exchange reaction and its variation among Hsp70 homologs, we measured the nucleotide exchange kinetics of homologs representing three Hsp70 subfamilies (see below): DnaK and HscA (Hsc66) of *E. coli* and human Hsc70.

Variation in nucleotide dissociation rates

We measured nucleotide dissociation rates directly, without or with physiological concentrations of P_i (20 mM), using fluorescent labeled N8-(4N′-methylanthraniloylaminobutyl)-8 aminoadenosine 5′-di/triphosphate (MABA-ADP and MABA-ATP). These analogs have affinities and kinetic properties similar to those of the authentic nucleotide interacting with DnaK[5], HscA and Hsc70 (not shown). Some kinetic properties were already established earlier and are similar to those determined here[5,7–9,15]. Commonly, all three proteins had dissociation rates for

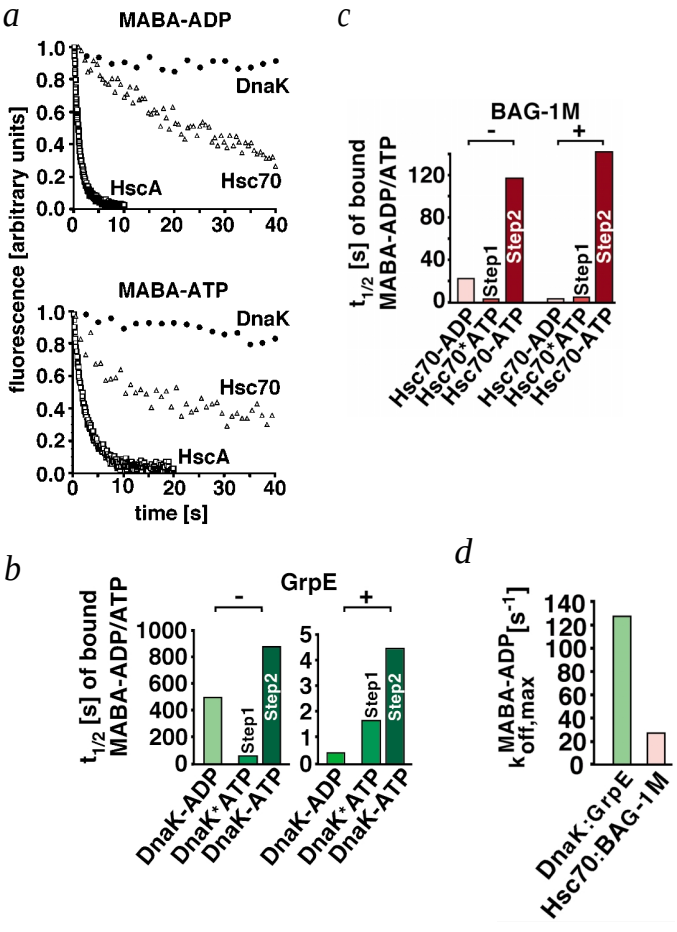

Fig. 1 Variability in nucleotide dissociation rates and utilization of exchanges factors. ***a***, Time courses of dissociation of MABA-ADP and MABA-ATP from *E. coli* DnaK, *E. coli* HscA and human Hsc70 in the presence of an excess of ATP and P_i. ***b***, Influence of GrpE on dissociation of MABA-ADP–DnaK and MABA-ATP–DnaK (initial encounter (step 1) and tightly bound (step 2)), shown as half-lives (s). ***c***, Influence of BAG-1M on dissociation of MABA-ADP–Hsc70 and MABA-ATP–Hsc70 (step 1, step 2) complexes shown as half lives. ***d***, Comparison of the maximal dissociation rates (s^{-1}) of MABA-ADP–DnaK by GrpE (taken from ref. 11) and MABA-ADP–Hsc70 by BAG-1M. Maximal MABA-ADP–Hsc70 dissociation rates were obtained by measuring the k_{off} (MABA-ADP) from Hsc70 with increasing amounts of BAG-1M

© 2001 Nature Publishing Group http://structbio.nature.com

Table 1 Hsp70 homologs differ in nucleotide exchange rates and exchange factors[1,2]

	k_{off}(ADP) (s^{-1})				k_{off}(ATP) (s^{-1}) step 1				k_{off}(ATP) (s^{-1}) step 2			
	–GrpE		+GrpE		–GrpE		+GrpE		–GrpE		+GrpE	
DnaK	0.0014	(495)	1.55	(0.5)	0.013	(54)	0.402	(1.7)	0.00077	(900)	0.15	(5)
Hsc70	0.0305	(23)	0.0307	(23)	0.214	(3.2)	nd[3]	nd[3]	0.0059	(117)	nd[3]	nd[3]
HscA	0.98	(0.7)	0.97	(0.7)	1.13	(0.6)	nd[3]	nd[3]	0.33	(2)	nd[3]	nd[3]
	–BAG-1M		+BAG-1M		–BAG-1M		+BAG-1M		–BAG-1M		+BAG-1M	
DnaK	0.0014	(495)	0.0014	(424)	0.013	(54)	nd[3]	nd[3]	0.00077	(900)	nd[3]	nd[3]
Hsc70	0.0305	(23)	0.32	(2.2)	0.214	(3.2)	0.174	(3.9)	0.0059	(117)	0.0052	(133)
HscA	0.98	(0.7)	0.98	(0.7)	1.13	(0.6)	nd[3]	nd[3]	0.33	(2)	nd[3]	nd[3]

[1]All rates represent at least six independent measurements in the presence of 20 mM P_i. Ratios of DnaK/Hsc70/HscA to GrpE and DnaK/Hsc70/HscA to BAG-1M were 1:4 and 1:2.
[2]All values in parenthesis are the corresponding half lives in s.
[3]nd, not determined.

MABA-ATP consistent with the biphasic association of MABA-ATP. Since the association of MABA-ATP is at least biphasic, one may assume that ATP association and dissociation follow the same kinetic route. Inorganic phosphate (20 mM) inhibited MABA-ADP dissociation of all three proteins by ~10-fold. Large differences exist between the absolute values of dissociation rates, with DnaK having the lowest and HscA the highest rates. The half life of the complex of DnaK with MABA-ADP+P_i is 495 s, whereas for Hsc70 it is 22-fold shorter and for HscA 700-fold shorter. The same trend exists for both dissociation reactions of MABA-ATP (Fig. 1, Table 1 for rates with P_i). The nucleotide dissociation reaction kinetics vary strongly within the Hsp70 family.

Selective utilization of nucleotide exchange factors

We investigated whether the homologs also differ in the interaction with exchange factors. As part of these experiments we determined whether the human Bag-1 homolog, Bag-1M, acts as nucleotide exchange factor for Hsc70, and whether GrpE and Bag-1M exhibit chaperone specificity. Gel filtration revealed that GrpE formed complexes with DnaK ($GrpE_2$–DnaK) but not with HscA and Hsc70. Instead, Bag-1M formed complexes with Hsc70 but not with DnaK and HscA (not shown).

Stopped-flow measurements revealed that GrpE stimulated nucleotide dissociation of DnaK but not of HscA and Hsc70. At four-fold molar excess over DnaK, GrpE stimulated dissociation of preformed DnaK–MABA-ADP complexes in the presence of P_i by 1,100-fold, consistent with earlier findings[11]. Interestingly, GrpE also strongly stimulated dissociation of MABA-ATP from DnaK by acting on both kinetic steps (33- and 191-fold for steps 1 and 2, respectively) (Fig. 1*b*). Therefore, GrpE does not distinguish the ADP-and ATP-bound states of DnaK.

Bag-1M only stimulated ADP dissociation from Hsc70 but not from DnaK and HscA (Table 1). In contrast to GrpE, Bag-1M did not stimulate dissociation of ATP (Fig. 1*c*). To determine its maximum potential as an exchange factor, we titrated increasing Bag-1M to a constant amount of pre-formed Hsc70–MABA-ADP complexes. Dissociation of the complexes was stimulated maximally by 110-fold (26.8 s^{-1}). Bag-1M is therefore a potent ADP exchange factor for Hsc70, and Bag-1M and GrpE exhibit strict selectivity for their Hsp70 partner.

Structural differences define three Hsp70 subfamilies

We searched for structural elements in the ATPase domains of the three homologs that may account for the differences in nucleotide exchange. We modeled the ATPase domains of 12 Hsp70 homologs (DnaK, HscA of *E. coli* and *Haemophilus influencae*; Ssc1, Ssa1, Ssb1 and Kar2 of *Saccharomyces cerevisiae*; mtHsp70, BiP of *Mus musculus*; Hsc70 of *Bos taurus* and *Homo sapiens*) on two atomic structures: the nucleotide-free ATPase domain of DnaK with open nucleotide binding cleft in complex with GrpE[16] and the ADP-bound ATPase domain of bovine Hsc70 with a closed cleft[17]. Although the modeled structures were almost completely superimposable, they differed in two previously unnoticed regions that allowed classification of the 12 homologs into three subfamilies with *E. coli* DnaK, *E. coli* HscA and human Hsc70 as prototypes. Sequence alignment of ~100 Hsp70 homologs confirmed that the entire Hsp70 family can be classified accordingly (not shown).

The first region is in an exposed loop in subdomain IIB near the nucleotide binding cleft (Fig. 2*a*). DnaK subfamily members share a particularly long loop (Ala 276–Arg 302 in *E. coli* DnaK) with subfamily-specific sequence and the ability to cooperate with GrpE homologs. Only a short segment of the loop (Pro 284–Ile 286) is close to GrpE in the $GrpE_2$–DnaK structure[16]. Given its positioning near the cleft, we speculated that it affects nucleotide exchange. Members of the Hsc70 subfamily share a loop with subfamily-specific sequence whose tip is four residues shorter, whereas members of the HscA subfamily share a less conserved, 10-residue shorter loop.

The second region is at the interface of the nucleotide binding cleft. In DnaK, we identified three conserved elements that may strengthen the interface and close the cleft: a hydrophobic patch (Met 259–Val 59 of DnaK) at the top of the cleft and two putative salt bridges (Glu 264–Arg 56, upper; Glu 267–Lys 55, lower) that are mainly responsible for the opposite charge distribution and, thereby, for the polarity of the interface (Fig. 2*c*,*d*). Interestingly, residues that constitute the hydrophobic patch and the upper salt bridge (Glu 264–Arg 56) seem to interact with GrpE[16]. GrpE loosens the ATPase interface by interfering with the hydrophobic contact and the salt bridges (Fig. 2*c*). In contrast, Hsc70 proteins lack a DnaK-like hydrophobic patch and the upper salt bridge, whereas HscA proteins lack all three elements. The classification of Hsp70 proteins based on the loop structure tightly correlates with the classification based on the three elements forming the subdomain interface.

Loop and salt bridges control nucleotide dissociation

To investigate their roles in nucleotide dissociation, we engineered DnaK variants step-by-step into Hsc70 and HscA with

© 2001 Nature Publishing Group http://structbio.nature.com

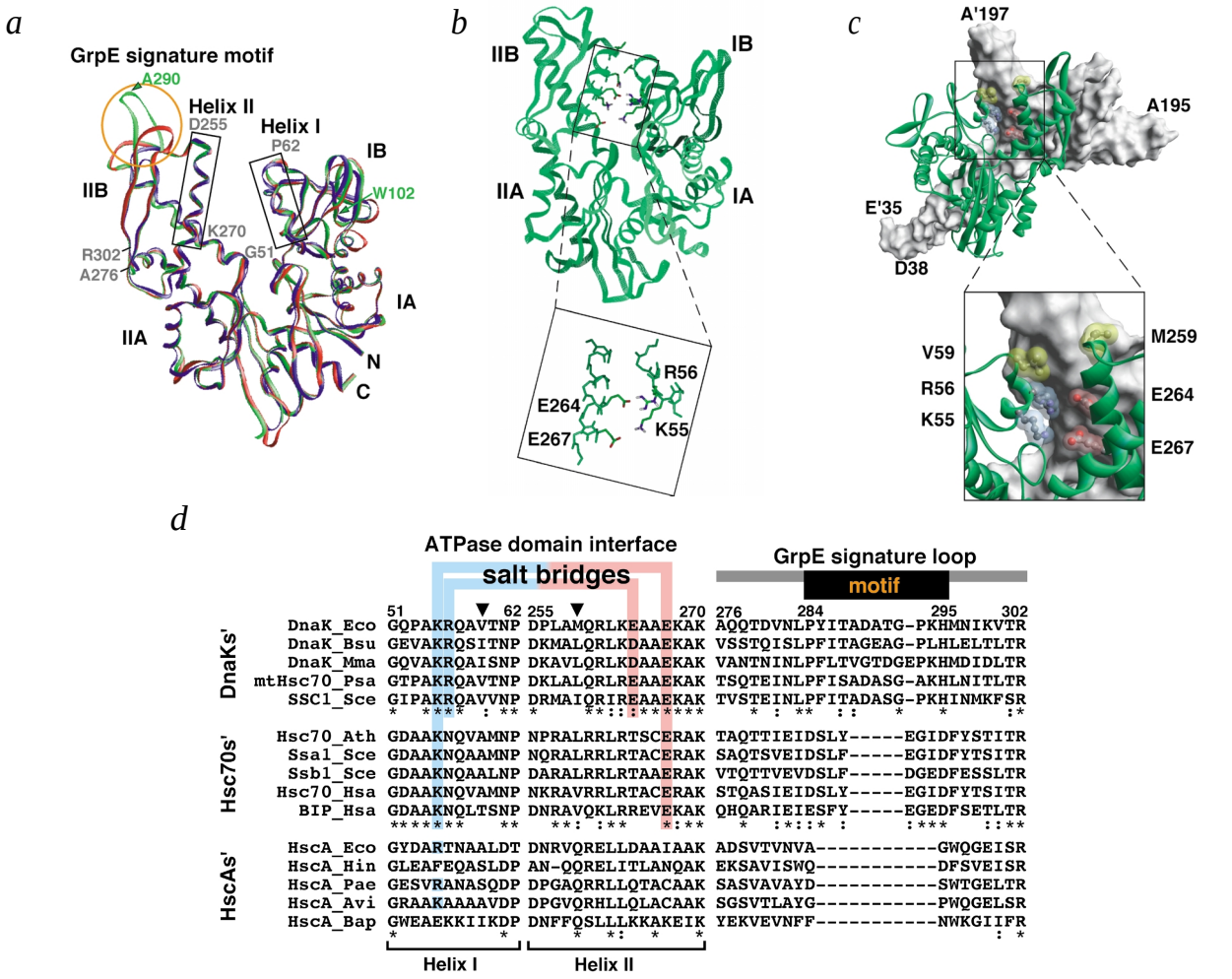

Fig. 2 Structural differences in the ATPase subdomains. ***a***, Superposition of the models of the ATPase domain of 12 Hsp70s. The exposed loop (Ala 276–Arg 302) in subdomain IIB and the interface of the nucleotide binding cleft, built up by Helix I (Gly 51–Pro 62) and Helix II (Asp 255–Lys 270), classify Hsp70 homologs into three subfamilies. Shown are four DnaK (green), six Hsc70 (red) and two HscA (blue) subfamily members. Green arrows point to Ala 290 of DnaK that was exchanged for cysteine and labeled with MIANS and to Trp 102 that was used for fluorescence energy transfer experiments. ***b***, Detailed view of the interface of the nucleotide binding cleft of *E. coli* DnaK in the ADP-bound conformation (modeled based on the structure of the ATPase domain of *B. taurus*, cocrystallized with ADP[17]), that visualizes the two putative salt bridges Glu 267–Lys 55 and Glu 264–Arg 56. ***c***, Position of the hydrophobic patch of residues M 259–Val 59, and the salt bridges Glu 264–Arg 56 and Glu 267–Arg 55 within the crystal structure of the ATPase domain of DnaK in open state cocrystallized with GrpE[16]. ***d***, Sequence alignment classifies Hsp70 family members according to identified structural differences in the ATPase domain. Sequences of the ATPase subdomain interfaces and loop segments of Hsp70 homologs were aligned according to the structures of *B. taurus* Hsc70 and *E. coli* DnaK. The evolutionary occurrence of the *E. coli* DnaK salt bridges Glu 267–Lys 55 and Glu 264–Arg 56 and hydrophobic interaction (M259–V59; black arrowheads) are visualized. The tip of the exposed loop (T287–G292) and its flanking regions (P284–I286, P292–H295), which are highly homologous within the DnaK subfamily, were termed GrpE signature motif. Eco: *E. coli*, Bsu: *Bacillus subtilis*, Mma: *Methanosarcina mazei*, Psa: *Pisum sativum*, Sce: *S. cerevisiae*, Ath: *Arabidopsis thaliana* Hsa: *H. sapiens*, Hin: *H. influenzae*, Pae: *Pseudomonas aeruginosa*, Avi: *Acetobacter vinelandii*, Bap: *Buchneria aphidicola*. The 'asterick' shows identity and 'colon' indicates similarity within the three subgroups. Structures made by Insight II and Webviewer 3.7. Sequence alignments and structure modeling were performed using Clustal W and SWISS-Model[27–29].

respect to the loop and salt bridges (DnaK-R56A; DnaK-K55A; DnaK-R56A/K55A; DnaK-Loop70; DnaK-Loop70/R56A; DnaK-LoopA; DnaK-LoopA/K55A/R56A). Because these alterations occur naturally within the Hsp70 family, they were not expected to perturb the local structure and the coupling mechanism between the ATPase and substrate binding domains. These assumptions were supported by circular dichroism, proteolysis and tryptophan fluorescence (data not shown).

The mutations had additive effects on nucleotide exchange of DnaK. For MABA-ADP, disruption of the upper (DnaK-R56A) or lower (DnaK-K55A) or both (DnaK-R56A/K55A) salt bridges decreased the half life of the complex by 2-, 6- and 9.3-fold, respectively, compared to wild type DnaK (495 s). Alterations in the loop also decreased its half life, by two-fold for DnaK-Loop70 and four-fold for DnaK-LoopA. Stronger changes occurred where the loop and salt bridge alterations were combined, with half lives decreasing three-fold for DnaK-Loop70/R56A (Hsc70-type) and 45-fold for DnaK-LoopA/K55A/R56A (HscA-type) (Fig. 3*a*). Both salt bridges and the loop therefore contribute individually and act synergistically to stabilize the DnaK–MABA-ADP complex. The hydrophobic contact is probably responsible for further five-fold stabilization, since the complex of MABA-ADP with Hsc70 (lacking this contact) is about five-fold less stable than

© 2001 Nature Publishing Group http://structbio.nature.com

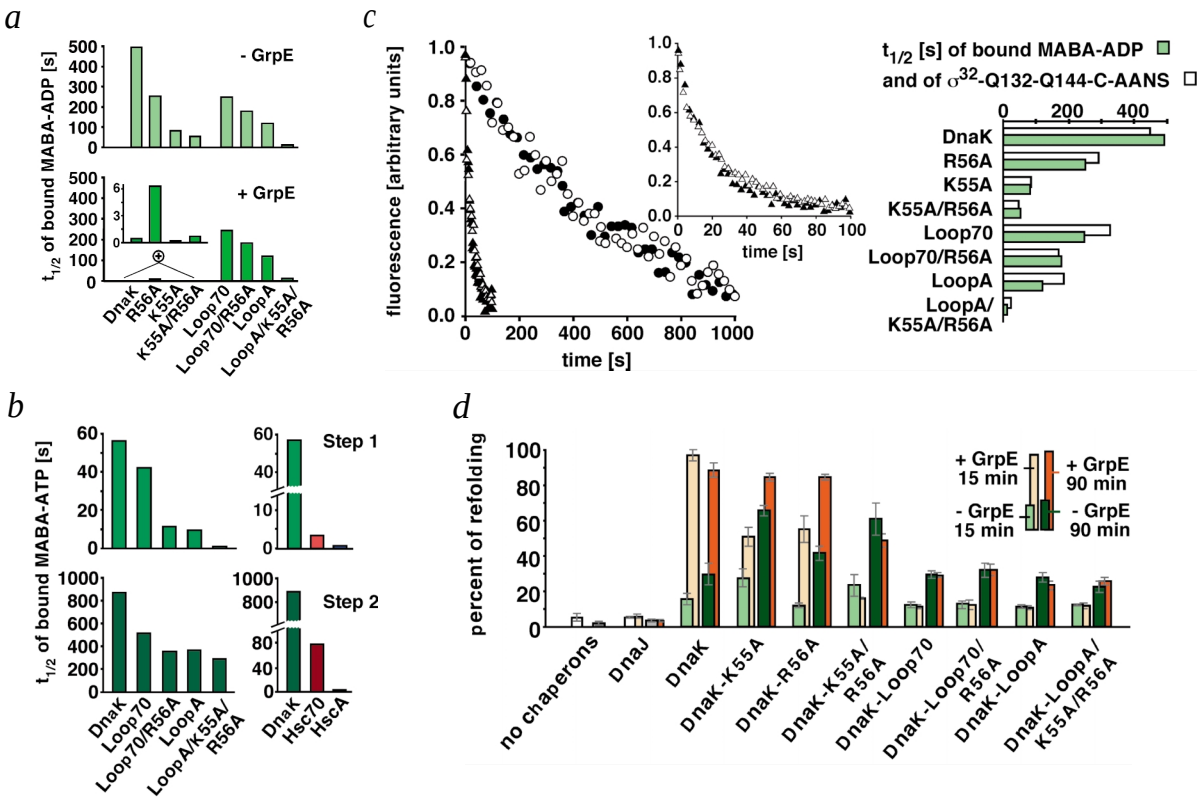

Fig. 3: Mutational alteration of the loop and salt bridges increases nucleotide dissociation rate and decreases chaperone activity of DnaK. ***a***, Comparison of the half life of the complexes of MABA-ADP with wild type and mutant DnaK proteins in absence or presence of GrpE. Experiments were performed in presence of P_i and a molar ratio of DnaK:GrpE of 1:4. ***b***, Comparison of the half lives of both complexes of MABA-ATP (step 1, step 2) with mutant and wild type DnaK, HscA and Hsc70. ***c***, Decay of the fluorescence signal of labeled peptide substrate (σ^{32}-Q132-Q144-C-AANS)[30] or MABA-ADP by dissociation from wild type DnaK and the DnaK-LoopA/K55A/R56A mutant protein in presence of P_i. Dissociation of MABA-ADP (solid circle) and peptide substrate (open circle) from DnaK(wt), and dissociation of MABA-ADP (solid triangle) and peptide (open triangle) from DnaK-LoopA/K55A/R56A mutant protein are represented. The bar graph summarizes the half lives for the complexes of MABA-ADP (green bars) and peptide substrate (white bars) with wild type and mutant DnaK proteins. ***d***, Refolding of firefly luciferase by wild type and mutant DnaK proteins and DnaJ in the absence or presence of GrpE. Bars represent refolding yields (percent of native firefly luciferase) in absence and presence of GrpE, respectively, at two time points (15 and 90 min) as indicated in the inset.

that complexed with DnaK-Loop70/R56A. Furthermore, Glu 267 of DnaK forms a hydrogen bond to the ribose of the nucleotide and may thereby stabilize the complex[17]. This residue is entirely conserved within the DnaK and Hsc70 subfamilies but is missing within the HscA subfamily, which may account for the even lower stability of the MABA-ADP complex with HscA.

For MABA-ATP dissociation, we analyzed the DnaK loop mutants with or without salt bridges (DnaK-Loop70, DnaK-Loop70/R56A, DnaK-LoopA and DnaK-LoopA/K55A/R56A). The alteration primarily affected the initial encounter DnaK*–ATP complex (Fig. 3*b*). Introduction of the Hsc70-type loop in the presence (DnaK-Loop70) or absence (DnaK-Loop70/R56A) of the upper salt bridge decreased its half life by 1.3- and 4.9-fold, respectively, compared to wild type DnaK. Introduction of the HscA-type loop in the presence (DnaK-LoopA) or absence (DnaK-LoopA/R56A-K55A) of both salt bridges decreased its half life by 6- and 56-fold, respectively. Thus, the loop and salt bridges act synergistically to prevent the dissociation of initially bound ATP (step 1). These elements also act during ATP association as they shift the equilibrium to the tightly bound DnaK-ATP state by stabilizing the transition from the nucleotide-free form to the loosely bound state (initial encounter DnaK*–ATP complex).

Our results show that the loop and salt bridges constitute a trap allowing rapid association of ATP and slow dissociation of ATP and ADP ± P_i. Mutation of these elements converted DnaK into Hsc70 and HscA with respect to nucleotide exchange. The salt bridges and the hydrophobic contacts might function to tightly close the nucleotide binding cleft. The role of the loop is less obvious. Given that the loop is exposed to the solvent, we speculate that it may reach over to subdomain IB of the ATPase domain of DnaK, thereby acting as a latch.

To support this hypothesis we performed fluorescence resonance energy transfer (FRET) experiments using Trp 102 in subdomain IB (Fig. 2*a*) as donor and 2-(4′-maleimidylanilino) naphthalene-6-sulfonic acid (MIANS) linked to a cysteine introduced at position 290 (DnaK-A290C) at the tip of the exposed loop as acceptor. To avoid the known interference of the substrate binding domain with tryptophan fluorescence[18], we used the isolated ATPase domain of DnaK for the FRET experiments. In the presence of MIANS, fluorescence of Trp 102 decreased at 344 nm compared to the unlabeled protein, while a fluorescence signal appeared at 424 nm (acceptor). The acceptor fluorescence signal was higher in the presence of ADP and ATP than in the absence of nucleotide. These data are consistent with our hypothesis of a nucleotide-dependent change of distance between the position 290 in the exposed loop and Trp 102 in subdomain IB (Fig. 2*a*).

© 2001 Nature Publishing Group http://structbio.nature.com

© 2001 Nature Publishing Group http://structbio.nature.com

© 2001 Nature Publishing Group http://structbio.nature.com

The loop is essential for interaction of GrpE with DnaK

We investigated whether these structural elements affect the ability of GrpE to interact with DnaK. Gel filtration revealed that the DnaK mutants with alterations in the salt bridges (DnaK-R56A, DnaK-K55A and DnaK-K55A/R56A) formed $GrpE_2$–DnaK complexes, whereas the DnaK mutant proteins with altered loop (DnaK-Loop70, DnaK-Loop70/R56A, DnaK-LoopA, DnaK-LoopA/K55A/R56A) failed to form complexes with GrpE, even at high GrpE concentrations. We conclude that the exposed loop tip, although not directly contacting GrpE in the crystallized $GrpE_2$–DnaK complex, is essential for physical interaction between DnaK and GrpE (Fig. 2*c*). The tip residues (Pro 284–His 295) are highly conserved within the DnaK subfamily and are therefore termed GrpE signature motif (Fig. 2*a*,*d*).

Salt bridges affect nucleotide exchange by GrpE

GrpE was unable to stimulate dissociation of MABA-ADP from the DnaK mutant proteins with altered loop structure (Fig. 3*a*). In contrast, GrpE was able to stimulate MABA-ADP dissociation, although with different efficiencies, from DnaK mutant proteins with altered salt bridges. At the tested concentration, GrpE stimulated MABA-ADP dissociation from DnaK-R56A by only 73-fold, as compared to 1,100-fold in the case of wild type DnaK (Fig. 3*a*). This decreased efficiency may result from Arg 56 and its salt bridge partner Glu 264 contacting GrpE. The R56A mutation may dislocate Glu 264, render it inaccessible for GrpE binding and thereby lower the affinity of GrpE for DnaK-R56A. GrpE stimulated MABA-ADP dissociation from DnaK-K55A by 2,600-fold (2.4-fold above wild type). This increased efficiency may result from reorientation of the salt bridge partner of Lys 55, Glu 267, which in wild type DnaK stabilizes the bound nucleotide[17]. Consistent with both proposals, GrpE stimulated MABA-ADP dissociation from the DnaK mutant protein lacking both salt bridges (DnaK-K55A/R56A) by an intermediate 700-fold. Thus, the effects of the single mutations (DnaK-K55A, DnaK-R56A) appear to cancel each other out in the double mutant (DnaK-K55A/R56A).

Loop and salt bridges affect chaperone activity

The consequences of the altered nucleotide exchange for the chaperone activity of DnaK were analyzed by three approaches. First, we determined the stability of complexes between DnaK mutant proteins and a fluorescently labeled peptide (σ^{32}-Q132-Q144-C-AANS)[19]. Dissociation rates of this peptide from preformed DnaK–ADP–peptide complexes were measured in presence of ATP and excess unlabeled peptide (σ^{32}-Q132-Q144). This allowed kinetic evaluation of the alterations on the crucial step in the functional cycle of DnaK in which bound ADP must be released before ATP can bind and trigger substrate release. For all proteins, the dissociation rates of bound peptide correlated tightly with their MABA-ADP dissociation rates (Fig. 3*c*).

Second, we determined the ability of the DnaK mutant proteins to complement the thermosensitive growth phenotype of *dnaK103(am)* and *ΔdnaK52* mutants. Both mutants lack DnaK activity but differ in the level of DnaJ due to deletion of the promotor of the *dnaK*, *dnaJ* operon in the *ΔdnaK52* mutants . This difference contributes to the higher thermosensitivity of *ΔdnaK52* mutants than *dnaK103(am)*. In *ΔdnaK52* mutants, only when wild type DnaK was produced from expression plasmids did growth occur on LB plates at 40 °C. In *dnaK103* mutant cells, production of DnaK mutant proteins with alterations in the loop also failed to complement growth at 42 °C, whereas all DnaK mutant proteins with alterations in the salt bridges complemented growth, although at a higher level of production. Thus, alterations in the loop produced a complete loss-of-function phenotype, whereas alterations in the salt bridges resulted in a weaker, partial loss-of-function phenotype.

Third, we tested the ability of the DnaK mutant proteins to assist DnaK-, DnaJ- and GrpE-dependent refolding of chemically denatured firefly luciferase[20,21]. Spontaneous refolding of luciferase was <5% of native control (Fig. 3*c*). In the presence of DnaK, DnaJ and GrpE, refolding was rapid and efficient, reaching ~90% of native control within five minutes in the presence of 20 mM of P_i. When GrpE was omitted, refolding was slower and inefficient, reaching <30% of native control. Replacement of wild type DnaK by DnaK-K55A and DnaK-R56A resulted in lower refolding rates and yields in the presence of GrpE, but in faster rates (DnaK-K55A) and higher yields (DnaK-K55A and DnaK-R56A) in the absence of GrpE. The DnaK-K55A/R56A double mutant showed an even larger decrease in refolding rate and yield in the presence of GrpE compared to the single mutants, but the refolding rates and yields of the double mutants were at least as the single mutant in the absence of GrpE. Thus, mutations of both salt bridges render the refolding reaction inefficient but independent of GrpE. The DnaK mutant poteins with alterations in the loop failed completely to assist in luciferase refolding, with or without GrpE. These *in vitro* phenotypes correlate well to those observed *in vivo*.

Conclusions

The small disturbances in the kinetics of nucleotide release and the subsequent substrate release were found sufficient to affect the chaperone activity of DnaK. Thus, fine-tuning the nucleotide exchange rate of the DnaK ATPase is functionally important and could be exploited for regulation of the chaperone activity *in vivo*. The Hsp70 family exhibits large variability in nucleotide exchange rates caused by subfamily-specific alterations in the interface of the nucleotide binding cleft and the exposed loop. We propose that when the lower salt bridge is present in a Hsp70 homolog, an exchange factor is required for catalyzing nucleotide dissociation. We show that GrpE is specific for DnaK proteins that display a subfamily-specific loop, and provide mechanistic insights into the mode of GrpE action. Bag-1M is a potent exchange factor specific for Hsc70. This high selectivity of exchange factors for Hsp70 partner contributes to the functional diversification of Hsp70 chaperone systems.

Note added in proof: While this manuscript was under review, two studies were reported that identify the NMR structure of the Bag-1 domain (Briknarová, K. et al. Nature Struct. Biol. 8, 349-352 (2001)) and the crystal structure of the complex between the Bag-1 domain and the ATPase domain of Hsc70 (Sondermann, H. et al. Science 291, 1553-1557 (2001)). These two studies provide clear structural evidence that Bag-1 acts as a nucleotide exchange factor for Hsc70 and are consistent with the biochemical evidence reported in the present manuscript.

Methods

Proteins. Site-directed mutagenesis was performed as described[22]. DnaK mutants with changes in the loop (DnaK-Loop70; DnaK-LoopA) were produced by sequence replacement of DnaK-284-PYITADATGPKHMNIKVT-301 by the corresponding sequence of human Hsc70 (285-DSLYEGIDFYTSIT-298) and *E. coli* HscA (289-AGWQGEIS-296). DnaK wild type and mutant proteins, and HscA, DnaJ, GrpE, Hsc70 and BAG-1M were expressed in the *ΔdnaK52* strain, BB1553 (ref. 23) and purified as described[14,24–26]. Bound nucleotide was removed as described[5]. The ATPase domain of DnaK-A290C mutant

© 2001 Nature Publishing Group http://structbio.nature.com

protein was prepared by papain digestion of the full-length protein and chromatographic purification as described[18].

Kinetic measurements. Kinetic measurements were performed as described[5,11] in 25 mM HEPES/KOH, pH 7.6, 50 mM KCl, 5 mM $MgCl_2$, +/– 20 mM K_2HPO_4/KH_2PO_4 at 30 °C. Dissociation rates of MABA-ADP and MABA-ATP (N8-(4-N′-methylanthraniloylaminobutyl)-8 amino-adenosine 5′-di/triphosphate) were determined as described[5] using a stopped flow apparatus (SX.18MV, Applied Photophysics). Luciferase refolding was determined as described[24] with 20 mM K_2HPO_4/KH_2PO_4 at 30 °C and a DnaK:DnaJ:GrpE:luciferase ratio of 20:2:5:1.

Fluorescence measurements. DnaK-A290C ATPase domain was labeled with 2-(4′-maleimidylanilino)naphthalene-6-sulfonic acid (MIANS, Molecular Probes) and purified according to the manufacturer's protocol. Emission spectra (300–600 nm) of unlabeled and MIANS-labeled DnaK-A290C ATPase domain in the absence and presence of ATP-free ADP and ATP were measured in a Perkin Elmer LS-50B spectrometer at 295 nm excitation wavelength.

Acknowledgments
We thank J. Höhfeld and R. Morimoto for plasmids expressing Bag-1M and Hsc70; A. Valencia and A. Buchberger for design and cloning of *dnaK-K55A*; T. Hesterkamp, A. Hoelz and T. Laufen for helpful discussions. This work was supported by grants of the DFG to J.R., and the DFG (Graduiertenkolleg Biochemie der Enzyme; Leibniz program) and the Fonds der Chemischen Industrie to B.B.

Correspondence should be addressed to B.B. *email: bukau@ruf.uni-freiburg.de*

Received 8 January, 2001; accepted 19 March, 2001.

1. Hartl, F.U. *Nature* **381**, 571–580 (1996).
2. Bukau, B. & Horwich, A.L. *Cell* **92**, 351–366 (1998).
3. Schmid, D., Baici, A., Gehring, H. & Christen, P. *Science* **263**, 971–973 (1994).
4. Mayer, M.P. *et al. Nature Struct. Biol.* **7**, 586–593 (2000).
5. Theyssen, H., Schuster, H.-P., Bukau, B. & Reinstein, J. *J. Mol. Biol.* **263**, 657–670 (1996).
6. Ha, J.-H. & McKay, D.B. *Biochemistry* **33**, 14625–14635 (1994).
7. Ha, J.-H. & McKay, D.B. *Biochemistry* **34**, 11635–11644 (1995).
8. Slepenkov, S.V. & Witt, S.N. *Biochemistry* **37**, 1015–1024 (1998).
9. Russell, R., Jordan, R. & McMacken, R. *Biochemistry* **37**, 596–607 (1998).
10. Liberek, K., Marszalek, J., Ang, D., Georgopoulos, C. & Zylicz, M. *Proc. Natl. Acad. Sci. USA* **88**, 2874–2878 (1991).
11. Packschies, L. *et al. Biochemistry* **36**, 3417–3422 (1997).
12. Bimston, D. *et al. EMBO J.* **17**, 6871–6878 (1998).
13. Takayama, S. *et al. EMBO J.* **16**, 4887–4896 (1997).
14. Höhfeld, J. & Jentsch, S. *EMBO J.* **16**, 6209–6216 (1997).
15. Silberg, J.J. & Vickery, L.E. *J. Biol. Chem.* **275**, 7779–7786 (2000).
16. Harrison, C.J., Hayer-Hartl, M., Di Liberto, M., Hartl, F.-U. & Kuriyan, J. *Science* **276**, 431–435 (1997).
17. Flaherty, K.M., Deluca-Flaherty, C. & McKay, D.B. *Nature* **346**, 623–628 (1990).
18. Buchberger, A. *et al. J. Biol. Chem.* **270**, 16903–16910 (1995).
19. McCarty, J.S. *et al. J. Mol. Biol.* **256**, 829–837 (1996).
20. Schröder, H., Langer, T., Hartl, F.-U. & Bukau, B. *EMBO J.* **12**, 4137–4144 (1993).
21. Szabo, A. *et al. Proc. Natl. Acad. Sci. USA* **91**, 10345–10349 (1994).
22. Kunkel, T.A., Bebenek, K. & McClary, J. *Methods. Enzymol.* **204**, 125–139 (1991).
23. Bukau, B. & Walker, G. *EMBO J.* **9**, 4027–4036 (1990).
24. Buchberger, A., Schröder, H., Büttner, M., Valencia, A. & Bukau, B. *Nature Struct. Biol.* **1**, 95–101 (1994).
25. Hesterkamp, T. & Bukau, B. *EMBO J.* **17**, 4818–4828 (1998).
26. Schönfeld, H.-J., Schmidt, D. & Zulauf, M. *Progr. Colloid. Polym. Sci.* **99**, 7–10 (1995).
27. Peitsch, M.C. *Bio/Technology* **13**, 658–660 (1995).
28. Peitsch, M.C. *Biochem. Soc. Trans.* **24**, 274–279 (1996).
29. Guex, N. & Peitsch, M.C. *Electrophoresis* **18**, 2714–2723 (1997).
30. McCarty, J.S., Buchberger, A., Reinstein, J. & Bukau, B. *J. Mol. Biol.* **249**, 126–137 (1995).

© 2001 Nature Publishing Group http://structbio.nature.com

Gal repressosome contains an antiparallel DNA loop

Mark Geanacopoulos[1], George Vasmatzis[2], Victor B. Zhurkin[3] and Sankar Adhya[1]

[1]Laboratory of Molecular Biology and [3]Laboratory of Experimental and Computational Biology, National Cancer Institute, National Institutes of Health, Bethesda, Maryland 20892, USA. [2]Mayo Clinic Cancer Center and Division of Experimental Pathology, Mayo Clinic, Rochester, Minnesota 55905, USA.

Gal repressosome assembly and repression of the *gal* operon in *Escherichia coli* occurs when two dimeric GalR proteins and the histone-like HU protein bind to cognate sites causing DNA looping. Structure-based genetic analysis defined the GalR surfaces interacting to form a stacked, V-shaped, tetrameric structure. Stereochemical models of the four possible DNA loops compatible with the GalR tetramer configuration were constructed using the sequence-dependent structural parameters of the interoperator DNA and conformation changes caused by GalR and asymmetric HU binding. Evaluation of their DNA elastic energies gave unambiguous preference to a loop structure in which the two *gal* operators adopt an antiparallel orientation causing undertwisting of DNA.

Nucleoprotein complexes comprising DNA loops play a critical role in the regulation of transcription[1,2] and many other cellular processes. Despite an ongoing effort to characterize DNA loop structures, our knowledge of any one remains incomplete largely because of their size, complexity and dependence on DNA topology. One such complex, the *Gal* repressosome, represses transcription of genes for galactose utilization in *Escherichia coli*. It forms when two dimeric GalR repressors bind to specific operator sites and when HU, an abundant component of the bacterial nucleoid, binds to a site between them[3]; negatively supercoiled DNA is absolutely required for repressosome assembly[4,5] (Fig. 1). Here, we report an innovative approach for determining the structure of this complex. First, genetic data were used to determine the overall orientation of the GalR dimers in a tetrameric structure. Next, empirically based modeling was employed to determine the trajectory of the DNA loop.

Mapping GalR surfaces by genetic analysis

To identify the domain of GalR involved in repressosome formation, we systematically altered the side chains of the surface-exposed residues without changing the protein's overall structure. In the absence of the X-ray diffraction structure, a homology model of GalR was constructed from the crystal structures of LacI and PurR, closely related members of the same family of DNA binding proteins[6]. In the model and in the X-ray crystal structures of seven GalR homologs, the highly conserved monomer consisted of two nearly identical subdomains, each containing five parallel β-sheets sandwiched between two layers of α-helices[6,7]. Site-directed amino acid substitutions in the GalR core were limited to residues predicted to be surface-exposed, making only nonconservative substitutions. To prevent disruption of overall structure, each residue was substituted with the amino acid occupying the corresponding position in LacI, PurR or GalS[8].

An *in vivo* assay examined the effect of the site-directed mutations on GalR function by using a dual reporter strain that enables measurement of the DNA binding activity of a GalR mutant separately from its ability to form the repressosome structure[6]. The reporter system makes use of the two differentially regulated *gal* promoters, *P1* and *P2*, fused to the *lacZ* and *gusA* genes, respective-